Prediction of motor outcome after acute stroke using rich-club organizational analysis

Lu Wang[1], Kui Kai Lau[3], Leonard SW Li[3], Yuen Kwun Wong[3], Christina Yau[4], Henry KF Mak[1,2], Edward S Hui[1,2,*]

[1] Department of Diagnostic Radiology, University of Hong Kong, Pokfulam, HKSAR

[2] State Key Laboratory of Brain and Cognitive Sciences, University of Hong Kong, Pokfulam, HKSAR

[3] Department of Medicine, University of Hong Kong, Pokfulam, HKSAR

[4] Department of Occupational Therapy, Tung Wah Hospital, HKSAR

[*] Corresponding author

Abstract

Stroke is one of the major diseases that causes disability, such as motor impairment. As a complex network of integrated regions, brain plasticity underlies functional recovery. Study showed that rich-club, highly connected and central brain regions, may underpin brain function and be associated with many brain disorders. In this study, we aim to explore rich-club organizational changes in the process of stroke recovery, and also the biomarkers that may help predict motor outcome. A cohort of 16 first-time acute ischemic stroke patients (11 males; mean age 65.8±11.0) were recruited. Structural brain networks were measured using T1-weighted imaging and diffusion tensor imaging within 1 week, and 1, 3 and 6 months after stroke. Motor functions were also assessed using Extremeity Fugl-Meyer Motor (UE-FM) and Barthel Index (BI) at the same time points. Changes in rich club organization and brain network topology, and their relations with motor outcome were investigated using Bayesian linear mixed model. The predictors of motor outcome were also investigated. Rich club regions and normalized rich club coefficient changed during the course of stroke recovery. Apart from clustering coefficient, the degree, strength, efficiency and betweenness centrality of each rich club region did not change with time after stroke. Temporal change in topological and rich-club metrics, including the mean degree, degree and mean strength of periphery regions, density of local connections, density ratio of feeder and local connections, communication cost ratio of rich club and capacity of rich club, were observed. The communication cost ratio and capacity of local connections were found to correlate with UE-FM and BI. The communication cost of rich connections and normalized rich club coefficient were found to be the predictors for UE-FM, whilst the density of local connections , normalized rich club coefficient, cost ratio and communication cost ratio of feeder connections were found to be the predictors for BI. Our

findings highlight the role of rich club organizational changes in the process of stroke recovery, and that network measures of rich club organization may potentially be the prognostic indicator of motor recovery after acute ischemic stroke.

Introduction

Around 80% of patients suffer from motor impairment after stroke.[1,2] Brain plasticity mechanisms, including activity-dependent rewiring and synapse strengthening, may likely underlie the recovery of brain functions.[3–6] Previous studies have investigated the relation between motor recovery after stroke and the structural connectivity of local pathways, such as corticospinal[7–10], alternate corticofugal[11,12], and corticocortical pathways[13–15]. The relation between motor recovery and structural connectivity of stroke patients have also been investigated by large-scale analysis of structural connectivity[18].

The neuroarchitecture of all types of brain regions can not only be understood at the local and global levels, as is usually performed, but also specific groups of brain regions and the relationship amongst them, known as rich-club organization[19,20]. Rich-club organization consists of brain regions that are closely connected, a.k.a. high centrality, which can dominant the entire brain network.[19] Rich club organization has been found in the brain of new-born, children and adult.[21–23] The bilateral frontoparietal regions and subcortical regions, including precuneus, superior frontal, parietal cortex, putamen, hippocampus and thalamus, formed rich club organization of healthy adults.[23] Rich club organization has been found to serve brain functions and regarded as the core of communication of the whole human brain[24,25]. The rich club organization of patients with schizophrenia[26], Huntington's disease[27] and Alzheimer's disease[28] was impaired.

Two prior studies have investigated the relation between motor outcome of stroke patients versus rich club metrics, such as the number of rich-club nodes affected by stroke[29] and another the number of rich-club nodes and path length[30]. Considering that there is a lack of the understanding of the longitudinal changes in the rich-club organization after stroke, and the relation between motor outcome and the thereof, we therefore aimed to investigate whether rich club organization would change over the course of first acute ischemic stroke recovery, and also to investigate the biomarkers that may predict motor recovery.

Materials and methods

Subjects and motor assessment

Stroke patients (n = 16; 11 male; mean age 65.8 ± 11.0; infarct side: 50% left) with first-time acute ischemic stroke were recruited between September 2015 and July 2018 with informed consent. MRI and assessment of motor functions were performed for at less than 1 week (n = 12), and 1 (n = 16), 3 (n = 13) and 6 (n = 9) months after acute stroke. Motor functions were examined by the Upper-Extremity Fugl-Meyer assessment (UE-FM) scale and Barthel index (BI). The UE-FM was developed to quantitatively assess the severity of motor impairment of upper extremity due to hemiplegic stroke, and is based on the well-defined stages of motor recovery[31]. BI was developed to quantitatively assess disability and functional outcome[32]. All patients received rehabilitation at the Acute Stroke Unit of Queen Mary Hospital after admission due to acute stroke. After an average of 5 days after admission, patients were transferred to the Stroke Rehabilitation Ward of Tung Wah Hospital for more intensive rehabilitation. All patient underwent conventional occupational rehabilitation therapy sessions, including activity of daily living training, upper limb functional training, cognitive perceptual training and functional task training. All procedures were carried out following operational guidelines of Human Research Ethics Committee, and all protocols were approved by the Institutional Review Board of the University of Hong Kong/Hospital Authority Hong Kong West Cluster.

Image acquisition

All MRI scans were performed using a 3.0 T MRI scanner (Achieva TX, Philips Healthcare, Best, The Netherlands) with body coil for excitation and 8-channel head coil for reception. Diffusion tensor imaging (DTI) data was performed using single-shot spin-echo echo planar imaging, consisting of non-diffusion-weighted image (b0) and diffusion-weighted images (DWIs) with b-values = 1000 s/mm^2 along 32 gradient directions, were acquired with the following parameters: TR/TE = 4000/81 ms, field of view = 230 × 230 mm2, reconstructed resolution = 3 × 3 mm2, 33 contiguous slices with thickness of 3 mm, SENSE factor = 2, number of averaging = 2, total scan time ≈ 5 minutes. TI-weighted images data were obtained by a 3D Magnetization Prepared-Rapid Gradient Echo (MPRAGE) with the following parameters: TR/TE/TI = 7/3.17/800 ms, field of view = 240 x 240 mm^2, reconstruction resolution = 1 x 1 x 1 mm3, 160 contiguous slices, scan time = 6 min 1 s.

Image pre-processing

All of the pre-processing procedures were performed by SPM12 (https://www.fil.ion.ucl.ac.uk/spm/). Head motion correction was performed by registering DWI to b0 images[33]. MPRAGE images were first reoriented taking anterior commissure[34] as the origin. The reoriented MPRAGE images were normalized to MNI152 template to obtain a transformation matrix M. MNI152 template was then inverse normalized to MPRAGE images by the inverse of the transformation matrix M^{-1}. The inverse normalized MNI152 template was non-linearly registered to diffusion-weighted imaging and a transformation matrix T was obtained. In this way, an inverse warping transformation from the standard space to the native DTI space can be obtained.

Network construction

Tractography: Diffusion tensor and diffusion metrics were obtained using the Diffusion Toolkit[32]. White matter tractography was obtained using the TrackVis (http://trackvis.org) with the algorithm of Fibre Assignment by Continuous Tracking (FACT)[36,37] with angle threshold of 45° and random seed of 32. To smooth the corners of the fibres, spline filter was applied. The results of streamlines were used to construct the structural brain network.

Network nodes definition: Automated Anatomical Labelling 2 (AAL2) atlas[38] in the standard space was inversely wrapped to the individual DTI native space according to M^{-1} and T obtained in image pre-processing. 94 Cortical regions (47 for each hemisphere) were obtained and each region was regarded as a node, of these 8 regions were excluded, namely left and right inferior occipital gyrus, left and right superior temporal pole, left and right middle temporal pole and left and right inferior temporal pole, due to variations in brain coverage.

Network link definition: UCLA Multimodal Connectivity package was used to calculate the number and the length of fibres between every two regions. Two regions were defined as connected regions if a fibre occurs between them. The link weight was defined as the fibre count between two regions.

Network topology metrics

MATLAB (2018b) and brain Connectivity Toolbox (https://sites.google.com/site/bctnet/) was used to calculate brain network topology metrics. The metrics included: (1) node degree, defined as the number of connected links of a node; (2) node strength, defined as the sum of the weight of connected links of a node; (3) local clustering coefficient, represented as connection property to neighbourhood of a node; (4) global efficiency, defined as the average inverse shortest path length in the network; (5) local efficiency, defined as the global efficiency

computed on node neighbourhoods; (6) node betweenness centrality, defined as the fraction of all shortest paths in the network that contain a given node.

Rich club organization

R language (3.6.0) was used to estimate rich club organization for each subject at each time point using a previously published method[16]. Weighted rich club coefficient was calculated by 4 steps. First, for each degree (k), a subnetwork was obtained by extracting nodes with degree more than k and links amongst them. Second, for each subnetwork, the number of links (n) and sum of weights of the links (W) was calculated. Then, the top n strongest weights of the whole network were summed. The weighted rich club coefficient of this subnetwork is subsequently calculated as follows:[39]

$$\varphi^{w}(\mathrm{k}) = \frac{W_{>k}}{\sum_{l=1}^{n} w_l^{ranked}},$$

where $W_{>k}$ represents weights of the links more than k and $\sum_{l=1}^{n} w_l^{ranked}$ sum of top n weights of links. However, nodes with lower degree in a network have lower possibilities of sharing links with each other by coincidence, even random networks generate increasing rich club coefficients as a function of increasing degree threshold k. To circumvent with this effect, 1,000 random networks with the same size and same degree distribution of the network of interest were generated. The average of the rich-club coefficients of the 1,000 random networks were calculated. The normalized rich-club coefficient of the network of interest is defined as[19,20]

$$\varphi_{norm} = \frac{\varphi_k}{\varphi_{random}}$$

A subnetwork is considered as a rich club organization when $\varphi_{norm}(k) > 1$[40,41].

A node is considered as a rich club node when k ={k_1, k_2, …, k_n}, in which the highest k was called highest rich club level. Each node of a rich club organization was given a score according to their highest rich club level. And then after averaging the score of nodes from all participates at the same time point, the top 8 nodes(i.e., 10% of all nodes) were selected as rich club nodes so that number of nodes used to construct the rich club organization avoid different average degree across subjects.

Node and Connection types

There are two types of nodes in a rich club organization, namely rich club nodes and peripheral nodes. On the other hand, there are three types of connections in a rich club organization, namely rich club connections (between rich club nodes), feeder connections (between rich club nodes and non–rich club nodes), and local connections (between non–rich club nodes).[42]

Network communication

Cost of a link was defined by product of its length and density (the count of streamlines between two brain regions). Communication cost was defined by the product of length and density based on their topological distance[42]. To calculate communication cost of three connections, first, the shortest paths between 84 nodes should be calculated. Then, each link of the shortest paths was divided into three categories (rich club, feeder and local connections). Next, calculate the communication cost of each link by length and density. Last, communication cost of three kind of connections can be obtained by summing the communication cost of links in each kind. The metric ratio of a certain connection kind was defined as the sum of metric of this certain kind divided by the total metric of the whole network. Communication cost/density ratio was defined as the communication cost ratio divided by density ratio, which was the weight of capacity[42].

Statistical analysis

Statistical analyses were performed by R Language (version 3.6.0) with the function lmer (https://cran.r-project.org/web/packages/lme4/lme4.pdf) and blmer (https://cran.rproject.org/web/packages/blme/blme.pdf). To simplify the statistical analyses on the local structural brain networks, the left and right hemispheres were flipped so that the left hemisphere always corresponded to the ipsilesional hemisphere. Due to attrition, some of the behavioural data, as well as imaging data, were not obtained. Imputation was thus performed on the behavioural data to increase the effective sample size for subsequent statistical analyses. For patient no. 2, 13 and 15, the behavioural data at 6 months after stroke were imputed from those at 3 months. Since patient no. 11 and 16 already made full recovery at the last follow up, full behavioural scores were assumed for the missing time points. After imputation, 10 patients had the behavioural data for all 4 time points. The imputed behavioural data were underlined in Table 1.

To handle data with an unequal number of longitudinal measures, a Bayesian linear mixed model (LMM)[43,44] was used as the main model in the current study so that a posteriori estimation can be maximized in a Bayesian setting. When necessary, linear mixed models were

followed by post hoc tests with Bonferroni corrections for multiple comparisons at $p < 0.05$. This study mainly investigated three aspects: (1) To test whether the motor outcome and network metrics changed with time. In this part, models are established with the motor outcome and network metrics as responses, time as fixed variable, each subject as random variable, and age and gender as covariates. (2) To test the correlation of metrics with motor outcome. In this part, models were established with motor assessment data as responses, network metric to be tested as fixed variable, each subject as random variable, and age and gender as covariates. (3) To find the biomarkers that may predict motor recovery. Models were established with the change of motor outcome (subtract the baseline motor outcome from motor outcome at other time points) as response, each subject as random variable, metric to be tested as fixed variable, and time, age and gender as covariates. After selecting the metrics that may be predictors of response. A linear mixed regression model was established by the method of step wise. In the whole study, a best fitting model was chosen by comparing models using Likelihood ratio test with the principle of the smaller AIC, the better the model[45]. Also, the simplest model was chosen when the gap of AIC values and likelihood ratio test result were small.

Table 1. The baseline demographics and assessment of motor impairment (upper-extremity Fugl-Meyer motor scale) and performance of activity of daily living (Barthel Index) of n = 16 patients.

	Upper-Extremity Fugl-Meyer Motor Scale (0 – 66)				Barthel Index (0 – 100)			
Patient	< 1 week	1 month	3 months	6 months	< 1 week	1 month	3 months	6 months
1	33	64	66	66	55	90	100	100
2	N.A.	63	63	63	N.A.	95	100	100
3	N.A.	5	14	18	N.A.	65	85	100
4	0	2	N.A.	N.A.	0	40	N.A.	N.A.
5	N.A.	31	40	49	N.A.	65	80	85
6	N.A.	48	62	63	N.A.	25	75	95
7	0	7	13	20	35	40	45	70
8	0	5	5	5	30	50	50	50
9	56	64	66	66	55	60	100	100
10	54	59	64	64	55	85	95	100
11	60	66	66	66	65	100	100	100
12	0	3	30	45	45	30	75	90
13	0	60	66	66	0	70	95	95
14	2	33	N.A.	N.A.	30	40	N.A.	N.A.
15	0	4	4	4	0	50	60	60
16	64	66	66	66	80	100	100	100

Results

Patient demographics

MRI and motor assessment were performed on 12, 16, 13 and 9 patients at within 1 week, 1, 3 and 6 months after first-time acute ischemic stroke, respectively, as shown in Table 1. Linear mixed model was used to test the fixed effect of time on motor function (UE-FM and BI) in the process of stroke recovery. UE-FM ($\beta_{time} = 3.47$; $\chi_1^2 = 13.68$, $p < 0.001$; **Figure** 1 A) and BI ($\beta_{time} = 7.94, \chi_1^2 = 28.31$, $p < 0.001$; Figure 1 A) significantly increased with time. Post hoc tests showed UE-FM at 1 ($p = 0.01$), 3 ($p < 0.001$) and 6 ($p < 0.001$) months after stroke were significantly higher than within 1 week after stroke. BI at 1, 3 and 6 ($p < 0.001$, all) months after stroke were significantly higher than within 1 week, and those at 3 and 6 ($p < 0.001$, all) months were significantly higher than 1 month.

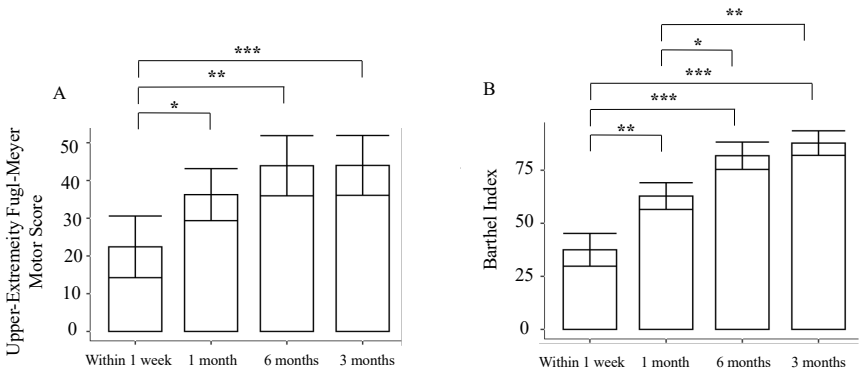

Figure 1. Box plot with error bar (standard deviance) of the upper-extremeity Fugl-Meyer motor score (A) and Barthel index (B) within 1 week (n = 12), 1 (n = 16), 3 (n = 13) and 6 (n = 9) months after first-time acute stroke. Post hoc tests with Bonferroni corrections for multiple comparisons of different time points were performed(*p <0.05, **p<0.01, ***p<0.001)

Development of rich club organization

The present research tracked the rich club organizational development of structural network of brain at 4 time points after stroke: within 1 week (**Figure 2 A**), 1 (**Figure 2 B**), 3 (**Figure 2 C**) and 6 months (**Figure 2 D**). Obvious rich-club organization was found from the structural brain network at different time points. Not each individual had normalized rich-club coefficient that was more than 1 in a wide range of degree except that at 6 months. For each time point, a list was obtained by averaging individual rich club nodes scores ranked in descending order by degree. The top 8 (10%) nodes of the list were selected to represent rich club regions at 4 time points and the other regions were identified as peripheral regions, which could ensure rich club organization established by equal numbers of nodes. The rich club regions at within 1 week

included: Frontal_Sup_2_L, Frontal_Sup_2_R, Supp_Motor_Area_L, Supp_Motor_Area_R, Insula_R, Cingulate_Ant_R, Cingulate_Mid_L Cingulate_Mid_R. At 1 month after stroke, Cingulate_Ant_L appeared in rich club regions and Supp_Motor_Area_L disappeared. At 3 months after stroke, Cingulate_Ant_L disappeared in rich club regions and Putamen_R appeared. Putamen_R disappeared and Insula_L first appeared in rich club regions at 6 months after stroke when subjects were functionally recovered.

Degree of $0 < k < 34$ was reported in this research according to the highest degree k more than 80% subjects had at all time points. For each degree of k, linear mixed model was used to test the effect of time on normalized rich club coefficient. Normalized rich club coefficient was affected by time when degree was in the range $28 < k < 33$ ($p<0.05$, the logic of the likelihood ratio test). Time showed significant effect on normalized rich club coefficient when k is equal to 20 ($\chi_1^2 = 7.22$, $p = 0.007$, $\beta_{time} = 0.010$), 21 ($\chi_1^2 = 6.87$, $p = 0.008$, $\beta_{time} = 0.011$), 22 ($\chi_1^2 = 6.83$, $p = 0.008$, $\beta_{time} = 0.013$), and 23 ($\chi_1^2 = 6.30$, $p = 0.012$, $\beta_{time} = 0.014$).

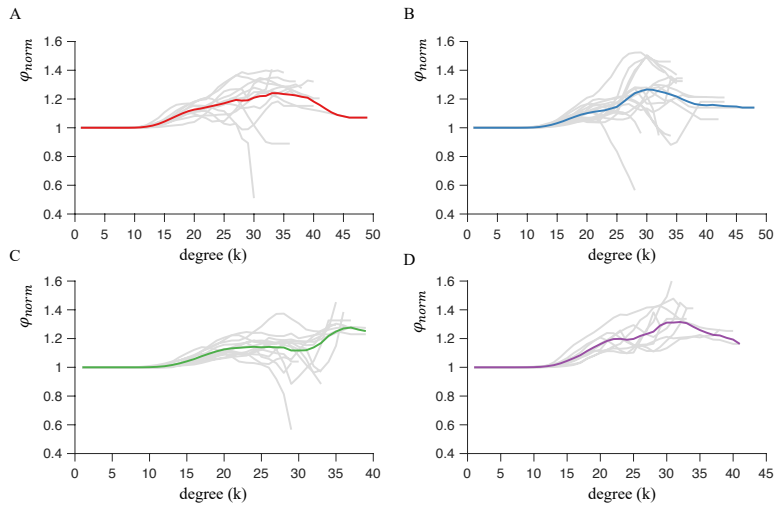

Figure 2. Mean normalized rich club coefficient curves (coloured lines) for the structural brain network at (A) within 1 week, (B) 1, (C) 3 and (D) 6 months after first-time acute stroke. Individual normalized rich-club curves are also shown in grey. Each individual and mean normalized rich club coefficients were larger than 1 in a range of k, suggesting rich club organization existed in all networks.

Development of network topological metrics

To explore the detail development of brain network, topological metrics were examined in regional scale, rich club scale, and large scale respectively. Regional scale means metric related to each node. Rich club scale means mean nodal metrics of rich club and periphery nodes, or

mean link metrics of rich, feeder and local connections. Large scale means the mean metrics of nodes of the whole brain network. Topological metrics in three scales were calculated including nodal degree, nodal strength, clustering coefficient, local efficiency, and betweenness centrality through the method referred in Materials and Methods. For each node, linear mixed model was used to test fixed effect of time on nodal scale metrics with age and gender as covariates, subject as random variable. 11 regions of nodal degree changed with time including Frontal_Sup_2_R, Frontal_Inf_Oper_L, Frontal_Sup_Medial_R, OFCmed_L, OFCmed_R, OFCant_L, OFClat_L, Parietal_Sup_L, SupraMarginal_L, Pallidum_R and Heschl_R (**Figure 3 A**). 14 regions of nodal strength changed with time including Rolandic_Oper_R, Frontal_Med_Orb_R, OFCmed_L, OFCmed_R, OFCant_L, OFCant_R, Insula_L, ParaHippocampal_L, Amygdala_R, Calcarine_R, Cuneus_R, Lingual_L, Lingual_R, Heschl_L (**Figure 3 B**). 3 regions of local clustering coefficient changed with time including Frontal_Sup_2_R, Supp_Motor_Area_L, Supp_Motor_Area_R and Frontal_Sup_Medial_R (**Figure 3 C**) 11 regions of local efficiency changed with time including Frontal_Inf_Oper_R , OFCant_L, OFCant_R, Insula_L, Hippocampus_L, ParaHippocampal_L, Lingual_L, Lingual_R, Caudate_L, Thalamus, Temporal_Sup_R (**Figure 3 D**). 6 regions of nodal betweenness centrality changed with time including Frontal_Sup_Medial_R , OFClat,Cingulate_Post_L, Lingual_R, Occipital_Mid_L, Postcentral_R (**Figure 3 E**).

Linear mixed model was used to test fixed effect of time on large scale and rich club scale metrics with gender and age as covariates and subject as random variable. Eight metrics changes were shown in Table 2. Time showed significant negative effect on mean degree ($\beta_{time} = -0.151, p = 0.008$), mean degree of peripheral nodes ($\beta_{time} = 0.145, p = 0.007$), mean strength of peripheral nodes (β_{time} = -0.119, $p = 0.049$), mean density of local connections ($\beta_{time} = -8.934$) and density ratio of local connections ($\beta_{time} = -0.005, p = 0.029$). While time showed positive effect on density ratio of feeder connections($\beta_{time} = 0.006, p = 0.008$), Communication cost ratio of rich connections ($\beta_{time} = 0.005, p = 0.020$) and ccommunication cost ratio/density ratio of rich connections ($\beta_{time} = 0.141, p = 0.023$).

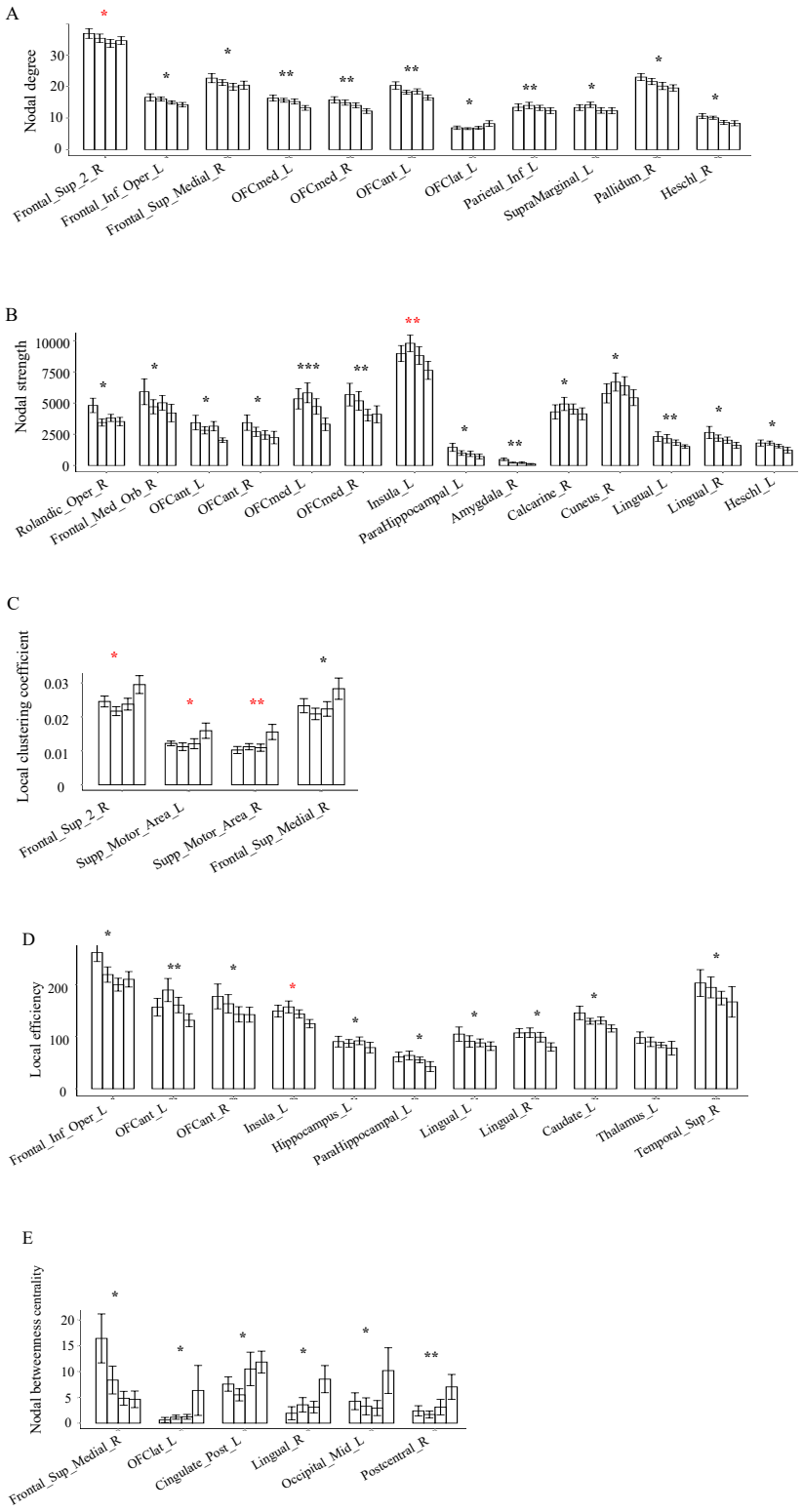

Figure 3. Regional brain network measures changes in the process of stroke recovery. A. Nodal degree B. Nodal Strength C. Local clustering coefficient D. Local efficiency E. Nodal betweenness centrality. Only regions with significance were displayed. *p<0.05, **p<0.01,***p<0.001. Red * represent rich club regions.

Table 2 Developmental time-related curves for different brain network metrics on large scale and rich club scale metrics. Only metrics with significance are shown.

Metric	β_0(intercept)	β_1(time)	Chisq	Chi Df	Pr(>Chisq)
DEG	20.641	-0.151	7.03	1	0.008
DEG_P	19.479	-0.145	7.30	1	0.007
STR_P	4.539	-0.119	3.86	1	0.049
DEN_L	281.802	-8.934	4.57	1	0.033
DEN_RF	0.293	0.006	7.06	1	0.008
DEN_RL	0.658	-0.005	4.74	1	0.029
COC_RR	0.021	0.005	5.43	1	0.020
COC_RR/DEN_RR	0.134	0.141	5.15	1	0.023

β_0, β_1 are the fixed effects coefficients: β_0 is the intercept, β_1 the linear slope; Chisq: Chi-square; Chi Df: Degree freedom of Chi-square; DEG_P: Mean degree of peripheral nodes; DTR_P: Mean strength of peripheral nodes; DEN_L: Mean density of local connections; DEN_RF: Density ratio of feeder connections; DEN_RL: Density ratio of local connections; COC_RR:Communication cost ratio of rich connections; COC_RR/DEN_RR: Communication cost ratio/density ratio of rich connections.

Correlations between motor behaviour and topological metrics and rich club metrics

Results of correlations between motor behaviour and topological metrics and rich club metrics were showed in Table 3. Communication cost ratio of local connection ($\beta = -72.81, p = 0.018; \beta = -133.30, p = 0.005;$ respectively), communication cost ratio/density ratio of local connections ($\beta = -41.21, p = 0.031;\ \beta = -64.11, p = 0.037;$ respectively) were found to correlated with both UE-FM and BI in the process of stroke recovery. In addition, mean clustering coefficient of peripheral nodes ($\beta = -1326.693, p = 0.047$), mean length of feeder and local connections ($\beta = -0.354, p = 0.034\ ; \beta = -0.197, p = 0.016,$ respectively) were found to be negative related with BI. Mean degree($\beta_{time} = 0.006, p = 0.008$) and mean degree of peripheral nodes ($\beta_{time} = 0.006, p = 0.008$) were found to be negative with UE-FM.

Table 3 Results of correlations between motor behaviour and topological metrics and rich club metrics

Results	Variable	β_0(intercept)	β_1(metric)	Chisq	Chi Df	Pr(>Chisq)
UE-FM	**DEG**	215.372	-6.583	5.772	1	0.016
	DEG_P	211.191	-6.761	5.333	1	0.021
	CC_RL	89.085	-72.811	5.617	1	0.018
	CC_RL/DEN_RL	87.838	-41.209	4.657	1	0.031

BI	**CLU_P**	198.711	-1326.693	3.947	1	0.047
	LEN_F	180.504	-0.354	4.478	1	0.034
	LEN_L	177.095	-0.197	5.838	1	0.016
	CC_RL	174.652	-133.299	7.856	1	0.005
	CC_RL/DEN_RL	170.42	-64.106	4.344	1	0.037

β_0, β_1 are the fixed effects coefficients: β_0 is the intercept, β_1 the linear slope; Chisq: Chi-square; Chi Df: Degree freedom of Chi-square; DEG : Mean degree; DEG_P: Mean degree of peripheral nodes; CLU_P: Mean clustering coefficient of peripheral nodes; LEN_f: Mean length of feeder connections; LEN_L: Mean length of local connections; CC_RR:Communication cost ratio of rich connections; CC_RR/DEN_RR: Communication cost ratio/density ratio of rich connections.

Motor behaviour prediction

Linear mixed models were used to explore communication metrics of brain network on the change of motor outcome(UE-FM and BI). Data of all points were used in the models. First, the factors correlated to change of motor outcome (subtract the baseline motor outcome from motor outcome at other time points) were selected by comparing the model with the metric and without the metric with each subject as random variable, metric to be tested as fixed variable, and time, age and gender as covariates. Communication cost of rich club ($\beta = -0.007, p = 0.031$) and normalized rich club coefficient were found to correlate with the change of UE-FM. Density of local connections($\beta = -0.173, p = 0.019$), cost ratio of feeder and local connections($\beta = 188.912, p = 0.016$; $\beta = -145.202, p = 0.025$), communication cost ratio of feeder and local connections($\beta = 492.186, p = 0.01$; $\beta = -337.023, p = 0.018$) and normalized rich club coefficients were found to correlate with the change of BI. Results were shown in **Table** 4. Variables were selected to prediction motor function as Table 5. Communication cost of rich connections and normalized rich club coefficient(k=21) can predict UE-FM change. Density of local connections, cost ratio of feeder connections, communication cost ratio of feeder connections can predict BI change.

Table 4 Communication metrics of brain network correlated the change of motor outcome

Motor outcome	Metric	β_0(intercept)	β_1(metric)	Chisq	Chi Df	Pr(>Chisq)
UE-FM	**COC_R**	-86.411	-0.007	4.634	1	0.031
	$\emptyset_{norm}$**(k=20)**	-286.141	159.564	4.497	1	0.034

	$\emptyset_{norm}$(k=21)	-349.076	210.436	7.858	1	0.005
	$\emptyset_{norm}$(k=22)	-272.152	149.048	5.486	1	0.019
	DEN_L	-69.432	-0.173	5.462	1	0.019
	CST_RF	-150.939	188.912	5.753	1	0.016
	CST_RL	10.797	-145.202	4.996	1	0.025
	COC_RF	-324.525	492.186	6.603	1	0.01
	COC_RL	70.354	-337.023	5.594	1	0.018
BI	$\emptyset_{norm}$(k=17)	-421.592	311.835	6.086	1	0.014
	$\emptyset_{norm}$(k=18)	-530.872	393.022	10.297	1	0.001
	$\emptyset_{norm}$(k=19)	-603.204	440.489	18.797	1	0
	$\emptyset_{norm}$(k=20)	-484.715	346.002	10.802	1	0.001
	$\emptyset_{norm}$(k=21)	-348.872	235.464	4.128	1	0.042
	$\emptyset_{norm}$(k=22)	-322.003	215.283	4.999	1	0.025
	$\emptyset_{norm}$(k=27)	-185.867	86.454	4.021	1	0.045

β_0, β_1 are the fixed effects coefficients: β_0 is the intercept, β_1 the linear slope; Chisq: Chi-square; Chi Df: Degree freedom of Chi-square; COC_R: Communication cost of rich club; DEN_L: Density of local connections; CST_RF: Cost ratio of feeder connections; CST_RL: Cost ratio of local connections; COC_RF:Communication cost ratio of feeder connections; COC_RL:Communication cost ratio of local connections.

Table 5 Summary of prediction models explored. Subtract of the follow-up outcome and initial outcome was defined as responses. Independent variables considered in the model were connected by '+'.

Response	Model	Variable	AIC	BIC	Chisq	Chi DF	Pr(>Chisq)
UE-FM – Initial UE-FM	**Baseline**	**Age + gender + time**	301	309.98			
	Prediction	**Age + gender + time + COC_R + $\emptyset_{norm}$(k=21)**	294.26	306.23	10.746	2	0.005
BI - Initial BI	**Baseline**	**Age+ gender+ time**	308.39	317.37			
	Prediction	**Age + gender + time + DEN_L + CST_RF + COC_RF + $\emptyset_{norm}$ (k19)**	297.62	314.08	20.775	5	<0.001

AIC: Akaike information criterion; BIC: Bayesian information criterion; logLik: log-likelihood Chisq: Chi-square; Chi Df: Degree freedom of Chi-square; COC_R: Communication cost of rich club; CST_RF: Cost ratio of feeder connections; COC_RF:Communication cost ratio of feeder connections

Discussion

The results show that rich club metrics can be prognostic indicator for motor recovery (UE-FM and BI) after acute ischemic stroke that did not found by studies previously. Our findings concerned the rich club regions, normalized rich club coefficient changes, and communication of the different connections to model and predict the motor outcome and it extend the work by Ktena[30] and Schirmer[29]. Ktena use the character path length and mean of NRC(the number of rich club regions influenced) to predict stroke recovery measured by National Institutes of Health Stroke Scale (NIHSS) and modified Rankin Scale (mRS) of 41 patients.[30] Schirmer investigated the association between the N_{RC} and stroke severity (NIHSS) and functional stroke outcome (mRS) of 344 patients. [29] They both showed the number of N_{RC} can be a potential predictor for prediction of stroke recovery. Out findings about the association between rich club metric and motor recovery suggest that larger scale metrics of connectivity is meaningful to predict motor recovery of stroke patients. Our studied first analysis the motor outcome based on rich club organization deeply and we calculated rich club organization by patients network, which can reflect rich club dynamics, however others identified those regions that are part of the rich-club as described by van den Heuvel and Sporns[52], which is another perspective in fact.

Motor recovery were found to increase with time, however, post-hoc test showed the motor at 3 month and 6 month after stroke were not significantly different, which confirmed a critical period of approximately 90 days of increased synaptic plasticity activated after stroke and at peak at 3 month after stroke[48,49]. It is normal that rich club organization changed in the process of stroke recovery because it is the backbone of brain communication[24,46,47] and as the patient recovered, brain structure changed because of plasticity including activity-dependent rewiring and synapse strengthening[48]. Among 4 time points, 75% rich club regions were stable including left and right dorsolateral superior frontal gyrus (No.3 and 4), right supplementary motor area (No.16), right insula (No.34), right anterior cingulate gyrus (No.36), left and right median cingulate gyrus (No.37 and 38. Regions changed including left supplementary motor area (No.15), left anterior cingulate gyrus(No.35), right putamen (No.78) and especially left insula

(No.33), which appeared at the last time point when patients functionally recovered. Among these 4 regions, three of them were left, which suggest that for rich club regions of the hemisphere of stroke region changed more than the other side. We found time showed significant effect on rich club coefficient when k was in the range of 20 to 23, which suggested rich club coefficient may have correlation with behaviour and it has been observed in Alzheimers' disease.[28]

Nodal analysis was performed in order to track the change of each region in detail and to see whether the rich club regions are infected. No rich club region were found to change in degree and betweenness centrality and only left insula in rich club regions were changed in strength and it is very different with Huntington's Disease[50], in which degree of rich club regions changed much. Three regions changed in clustering coefficient were all rich club regions including right dorsolateral superior frontal gyrus left and right supplementary motor area. It seems that clustering coefficient play an important role in function recovery.

Among four metric correlated with UE-FM and fiver metric correlated with BI, higher communication cost ratio and higher capacity of local connections were found to correlate with lower UE-FM and BI. Though other metrics were also found correlated with UE-FM including degree, degree of peripheral nodes, corelated with BI including clustering coefficient of peripheral nodes, length of feeder and local connections, the same metrics may release the inner basis of motor function essentially. Communication cost of rich connections and normalized rich club coefficient(k=21) can predict UE-FM change. Density of local connections, cost ratio of feeder connections, communication cost ratio of feeder connections can predict BI change.

Several limitations still need to be taken into consideration when interpreting the results. First, infract side of stroke lesion were different among the 16 patients. Stroke lesions of 8 patients were in left side and others were in right side. In order to avoid systematic error, we flipped all the brain regions of the patients whose stroke lesion infract side was right to left to ensure lesions in the same side, namely left side. However, it may influence the results slightly because the left and right hemisphere are not totally same, for example, the strength of left and right are not completely equal[52]. Second, Missing values existed in our dataset. In the longitude dataset collection, sometimes patients cannot come to perform MRI experiment because of their own individual regions. Only all patients attended to the MRI experiment at 1 month after stroke, and 4, 3, 7 patients unattended at within 1 week, 3 and 6 months after acute stroke respectively, which could reduce the quantality of the result. Third, when analysing the dataset, we found

411 sometimes there exited nonlinear tend of the data with time went by, which could be explored
412 in our future study.
413

References

(1) Langhorne, P.; Coupar, F.; Pollock, A. Motor Recovery after Stroke: A Systematic Review. *The Lancet Neurology* **2009**, *8* (8), 741–754.

(2) Warlow, C. P.; Van Gijn, J.; Dennis, M. S.; Wardlaw, J. M.; Bamford, J. M.; Hankey, G. J.; Sandercock, P. A.; Rinkel, G.; Langhorne, P.; Sudlow, C. *Stroke: Practical Management*; John Wiley & Sons, 2011.

(3) Johansson, B. B. Brain Plasticity and Stroke Rehabilitation: The Willis Lecture. *Stroke* **2000**, *31* (1), 223–230.

(4) Murphy, T. H.; Corbett, D. Plasticity during Stroke Recovery: From Synapse to Behaviour. *Nature Reviews Neuroscience* **2009**, *10* (12), 861–872.

(5) Schaechter, J. D. Motor Rehabilitation and Brain Plasticity after Hemiparetic Stroke. *Progress in neurobiology* **2004**, *73* (1), 61–72.

(6) Di Pino, G.; Pellegrino, G.; Assenza, G.; Capone, F.; Ferreri, F.; Formica, D.; Ranieri, F.; Tombini, M.; Ziemann, U.; Rothwell, J. C. Modulation of Brain Plasticity in Stroke: A Novel Model for Neurorehabilitation. *Nature Reviews Neurology* **2014**, *10* (10), 597–608.

(7) Ward, N. S.; Newton, J. M.; Swayne, O. B.; Lee, L.; Thompson, A. J.; Greenwood, R. J.; Rothwell, J. C.; Frackowiak, R. S. Motor System Activation after Subcortical Stroke Depends on Corticospinal System Integrity. *Brain* **2006**, *129* (3), 809–819.

(8) Kirton, A.; Shroff, M.; Visvanathan, T.; Deveber, G. Quantified Corticospinal Tract Diffusion Restriction Predicts Neonatal Stroke Outcome. *Stroke* **2007**, *38* (3), 974–980.

(9) Stinear, C. M.; Barber, P. A.; Smale, P. R.; Coxon, J. P.; Fleming, M. K.; Byblow, W. D. Functional Potential in Chronic Stroke Patients Depends on Corticospinal Tract Integrity. *Brain* **2007**, *130* (1), 170–180.

(10) Zhu, L. L.; Lindenberg, R.; Alexander, M. P.; Schlaug, G. Lesion Load of the Corticospinal Tract Predicts Motor Impairment in Chronic Stroke. *Stroke* **2010**, *41* (5), 910–915.

(11) Newton, J. M.; Ward, N. S.; Parker, G. J.; Deichmann, R.; Alexander, D. C.; Friston, K. J.; Frackowiak, R. S. Non-Invasive Mapping of Corticofugal Fibres from Multiple Motor Areas—Relevance to Stroke Recovery. *Brain* **2006**, *129* (7), 1844–1858.

(12) Lindberg, P. G.; Skejø, P. H.; Rounis, E.; Nagy, Z.; Schmitz, C.; Wernegren, H.; Bring, A.; Engardt, M.; Forssberg, H.; Borg, J. Wallerian Degeneration of the Corticofugal Tracts in Chronic Stroke: A Pilot Study Relating Diffusion Tensor Imaging,

Transcranial Magnetic Stimulation, and Hand Function. *Neurorehabilitation and neural repair* **2007**, *21* (6), 551–560.

(13) Strens, L. H. A.; Asselman, P.; Pogosyan, A.; Loukas, C.; Thompson, A. J.; Brown, P. Corticocortical Coupling in Chronic Stroke: Its Relevance to Recovery. *Neurology* **2004**, *63* (3), 475–484.

(14) Feydy, A.; Carlier, R.; Roby-Brami, A.; Bussel, B.; Cazalis, F.; Pierot, L.; Burnod, Y.; Maier, M. A. Longitudinal Study of Motor Recovery after Stroke: Recruitment and Focusing of Brain Activation. *Stroke* **2002**, *33* (6), 1610–1617.

(15) Schulz, R.; Braass, H.; Liuzzi, G.; Hoerniss, V.; Lechner, P.; Gerloff, C.; Hummel, F. C. White Matter Integrity of Premotor–Motor Connections Is Associated with Motor Output in Chronic Stroke Patients. *NeuroImage: Clinical* **2015**, *7*, 82–86.

(16) Rubinov, M.; Sporns, O. Complex Network Measures of Brain Connectivity: Uses and Interpretations. *Neuroimage* **2010**, *52* (3), 1059–1069.

(17) Fornito, A.; Zalesky, A.; Bullmore, E. *Fundamentals of Brain Network Analysis*; Academic Press, 2016.

(18) Crofts, J. J.; Higham, D. J.; Bosnell, R.; Jbabdi, S.; Matthews, P. M.; Behrens, T. E. J.; Johansen-Berg, H. Network Analysis Detects Changes in the Contralesional Hemisphere Following Stroke. *Neuroimage* **2011**, *54* (1), 161–169.

(19) Colizza, V.; Flammini, A.; Serrano, M. A.; Vespignani, A. Detecting Rich-Club Ordering in Complex Networks. *Nature physics* **2006**, *2* (2), 110.

(20) McAuley, J. J.; da Fontoura Costa, L.; Caetano, T. S. Rich-Club Phenomenon across Complex Network Hierarchies. *Applied Physics Letters* **2007**, *91* (8), 084103.

(21) Grayson, D. S.; Ray, S.; Carpenter, S.; Iyer, S.; Dias, T. G. C.; Stevens, C.; Nigg, J. T.; Fair, D. A. Structural and Functional Rich Club Organization of the Brain in Children and Adults. *PloS one* **2014**, *9* (2).

(22) Ball, G.; Aljabar, P.; Zebari, S.; Tusor, N.; Arichi, T.; Merchant, N.; Robinson, E. C.; Ogundipe, E.; Rueckert, D.; Edwards, A. D. Rich-Club Organization of the Newborn Human Brain. *Proceedings of the National Academy of Sciences* **2014**, *111* (20), 7456–7461.

(23) Van Den Heuvel, M. P.; Sporns, O. Rich-Club Organization of the Human Connectome. *Journal of Neuroscience* **2011**, *31* (44), 15775–15786.

(24) van den Heuvel, M. P.; Kahn, R. S.; Goñi, J.; Sporns, O. High-Cost, High-Capacity Backbone for Global Brain Communication. *Proceedings of the National Academy of Sciences* **2012**, *109* (28), 11372–11377.

(25) Senden, M.; Deco, G.; de Reus, M. A.; Goebel, R.; van den Heuvel, M. P. Rich Club Organization Supports a Diverse Set of Functional Network Configurations. *Neuroimage* **2014**, *96*, 174–182.

(26) van den Heuvel, M. P.; Sporns, O.; Collin, G.; Scheewe, T.; Mandl, R. C.; Cahn, W.; Goñi, J.; Pol, H. E. H.; Kahn, R. S. Abnormal Rich Club Organization and Functional Brain Dynamics in Schizophrenia. *JAMA psychiatry* **2013**, *70* (8), 783–792.

(27) McColgan, P.; Seunarine, K. K.; Razi, A.; Cole, J. H.; Gregory, S.; Durr, A.; Roos, R. A.; Stout, J. C.; Landwehrmeyer, B.; Scahill, R. I. Selective Vulnerability of Rich Club Brain Regions Is an Organizational Principle of Structural Connectivity Loss in Huntington's Disease. *Brain* **2015**, *138* (11), 3327–3344.

(28) Yan, T.; Wang, W.; Yang, L.; Chen, K.; Chen, R.; Han, Y. Rich Club Disturbances of the Human Connectome from Subjective Cognitive Decline to Alzheimer's Disease. *Theranostics* **2018**, *8* (12), 3237.

(29) Schirmer, M. D.; Ktena, S. I.; Nardin, M. J.; Donahue, K. L.; Giese, A.-K.; Etherton, M.; Wu, O.; Rost, N. Rich-Club Organization: An Important Determinant of Functional Outcome after Acute Ischemic Stroke. *Frontiers in neurology* **2019**, *10*, 956.

(30) Ktena, S. I.; Schirmer, M. D.; Etherton, M. R.; Giese, A.-K.; Tuozzo, C.; Mills, B. B.; Rueckert, D.; Wu, O.; Rost, N. S. Brain Connectivity Measures Improve Modeling of Functional Outcome after Acute Ischemic Stroke. *Stroke* **2019**, *50* (10), 2761–2767.

(31) Sullivan, K. J.; Tilson, J. K.; Cen, S. Y.; Rose, D. K.; Hershberg, J.; Correa, A.; Gallichio, J.; McLeod, M.; Moore, C.; Wu, S. S. Fugl-Meyer Assessment of Sensorimotor Function after Stroke: Standardized Training Procedure for Clinical Practice and Clinical Trials. *Stroke* **2011**, *42* (2), 427–432.

(32) Kwakkel, G.; Veerbeek, J. M.; Harmeling-van der Wel, B. C.; van Wegen, E.; Kollen, B. J. Diagnostic Accuracy of the Barthel Index for Measuring Activities of Daily Living Outcome after Ischemic Hemispheric Stroke: Does Early Poststroke Timing of Assessment Matter? *Stroke* **2011**, *42* (2), 342–346.

(33) Andersson, J. L.; Skare, S. A Model-Based Method for Retrospective Correction of Geometric Distortions in Diffusion-Weighted EPI. *Neuroimage* **2002**, *16* (1), 177–199.

(34) Talairach, J. 3-Dimensional Proportional System; an Approach to Cerebral Imaging. Co-Planar Stereotaxic Atlas of the Human Brain. *Thieme* **1988**, 1–122.

514 (35) Wang, R.; Benner, T.; Sorensen, A. G.; Wedeen, V. J. Diffusion Toolkit: A Software
515 Package for Diffusion Imaging Data Processing and Tractography. In *Proc Intl Soc*
516 *Mag Reson Med*; Berlin, 2007; Vol. 15.
517 (36) Mori, S.; Crain, B. J.; Chacko, V. P.; Van Zijl, P. C. Three-Dimensional Tracking of
518 Axonal Projections in the Brain by Magnetic Resonance Imaging. *Annals of*
519 *Neurology: Official Journal of the American Neurological Association and the Child*
520 *Neurology Society* **1999**, *45* (2), 265–269.
521 (37) Mori, S.; Van Zijl, P. C. Fiber Tracking: Principles and Strategies–a Technical Review.
522 *NMR in Biomedicine: An International Journal Devoted to the Development and*
523 *Application of Magnetic Resonance In Vivo* **2002**, *15* (7–8), 468–480.
524 (38) Rolls, E. T.; Joliot, M.; Tzourio-Mazoyer, N. Implementation of a New Parcellation of
525 the Orbitofrontal Cortex in the Automated Anatomical Labeling Atlas. *Neuroimage*
526 **2015**, *122*, 1–5.
527 (39) Opsahl, T.; Colizza, V.; Panzarasa, P.; Ramasco, J. J. Prominence and Control: The
528 Weighted Rich-Club Effect. *Physical review letters* **2008**, *101* (16), 168702.
529 (40) Ball, G.; Aljabar, P.; Zebari, S.; Tusor, N.; Arichi, T.; Merchant, N.; Robinson, E. C.;
530 Ogundipe, E.; Rueckert, D.; Edwards, A. D. Rich-Club Organization of the Newborn
531 Human Brain. *Proceedings of the National Academy of Sciences* **2014**, *111* (20), 7456–
532 7461.
533 (41) Bullmore, E.; Vértes, P. From Lichtheim to Rich Club: Brain Networks and Psychiatry.
534 *JAMA psychiatry* **2013**, *70* (8), 780–782.
535 (42) van den Heuvel, M. P.; Kahn, R. S.; Goñi, J.; Sporns, O. High-Cost, High-Capacity
536 Backbone for Global Brain Communication. *Proceedings of the National Academy of*
537 *Sciences* **2012**, *109* (28), 11372–11377.
538 (43) Cnaan, A.; Laird, N. M.; Slasor, P. Using the General Linear Mixed Model to Analyse
539 Unbalanced Repeated Measures and Longitudinal Data. *Statistics in medicine* **1997**, *16*
540 (20), 2349–2380.
541 (44) Verbeke, G.; Molenberghs, G. *Linear Mixed Models for Longitudinal Data*; Springer
542 Science & Business Media, 2009.
543 (45) Winter, B. Linear Models and Linear Mixed Effects Models in R with Linguistic
544 Applications. *arXiv preprint arXiv:1308.5499* **2013**.
545 (46) Harriger, L.; Van Den Heuvel, M. P.; Sporns, O. Rich Club Organization of Macaque
546 Cerebral Cortex and Its Role in Network Communication. *PloS one* **2012**, *7* (9),
547 e46497.

548 (47) de Reus, M. A.; van den Heuvel, M. P. Rich Club Organization and Intermodule
549 Communication in the Cat Connectome. *Journal of Neuroscience* **2013**, *33* (32),
550 12929–12939.
551 (48) Murphy, T. H.; Corbett, D. Plasticity during Stroke Recovery: From Synapse to
552 Behaviour. *Nature Reviews Neuroscience* **2009**, *10* (12), 861.
553 (49) Maulden, S. A.; Gassaway, J.; Horn, S. D.; Smout, R. J.; DeJong, G. Timing of
554 Initiation of Rehabilitation after Stroke. *Archives of physical medicine and*
555 *rehabilitation* **2005**, *86* (12), 34–40.
556 (50) McColgan, P.; Seunarine, K. K.; Razi, A.; Cole, J. H.; Gregory, S.; Durr, A.; Roos, R.
557 A.; Stout, J. C.; Landwehrmeyer, B.; Scahill, R. I. Selective Vulnerability of Rich Club
558 Brain Regions Is an Organizational Principle of Structural Connectivity Loss in
559 Huntington's Disease. *Brain* **2015**, *138* (11), 3327–3344.
560 (51) Schirmer, M. D.; Ktena, S. I.; Nardin, M. J.; Donahue, K. L.; Giese, A.-K.; Etherton, M.
561 R.; Wu, O.; Rost, N. S. Rich-Club Organization: An Important Determinant of
562 Functional Outcome after Acute Ischemic Stroke. *BioRxiv* **2019**, 545897.
563 (52) Van Den Heuvel, M. P.; Sporns, O. Rich-Club Organization of the Human Connectome.
564 *Journal of Neuroscience* **2011**, *31* (44), 15775–15786.
565
566
567